IOP PUBLISHING PHYSICS IN MEDICINE AND BIOLOGY

Phys. Med. Biol. **53** (2008) 361–373 doi:10.1088/0031-9155/53/2/005

Measurement of electric fields induced in a human subject due to natural movements in static magnetic fields or exposure to alternating magnetic field gradients

P M Glover and R Bowtell

The Sir Peter Mansfield Magnetic Resonance, Centre School of Physics and Astronomy, University of Nottingham, NG7 2RD Nottingham, UK

Received 27 September 2007, in final form 4 December 2007
Published 28 December 2007
Online at stacks.iop.org/PMB/53/361

Abstract

A dual dipole electric field probe has been used to measure surface electric fields *in vivo* on a human subject over a frequency range of 0.1–800 Hz. The low-frequency electric fields were induced by natural body movements such as walking and turning in the fringe magnetic fields of a 3 T magnetic resonance whole-body scanner. The rate-of-change of magnetic field (dB/dt) was also recorded simultaneously by using three orthogonal search coils positioned near to the location of the electric field probe. Rates-of-change of magnetic field for natural body rotations were found to exceed 1 T s^{-1} near the end of the magnet bore. Typical electric fields measured on the upper abdomen, head and across the tongue for 1 T s^{-1} rate of change of magnetic field were 0.15 $\pm$ 0.02, 0.077 $\pm$ 0.003 and 0.015 $\pm$ 0.002 V m^{-1} respectively. Electric fields on the abdomen and chest were measured during an echo-planar sequence with the subject positioned within the scanner. With the scanner rate-of-change of gradient set to 10 T m^{-1} s^{-1} the measured rate-of-change of magnetic field was 2.2 $\pm$ 0.1 T s^{-1} and the peak electric field was 0.30 $\pm$ 0.01 V m^{-1} on the chest. The values of induced electric field can be related to dB/dt by a 'geometry factor' for a given subject and sensor position. Typical values of this factor for the abdomen or chest (for measured surface electric fields) lie in the range of 0.10–0.18 m. The measured values of electric field are consistent with currently available numerical modelling results for movement in static magnetic fields and exposure to switched magnetic field gradients.

(Some figures in this article are in colour only in the electronic version)

Introduction

Since the earliest days of magnetic resonance imaging (MRI) researchers have been aware of issues surrounding the safety of this procedure (Mansfield and Morris 1982, McRobbie and Foster 1984, Schenck *et al* 1983). Although the patient safety issues surrounding the specific absorption rate (SAR) for radio-frequencies have been investigated in more detail, bio-effects of low-frequency magnetic field variation are still not well understood (Chakeres and de Vocht 2005, Kangarlu *et al* 1999, Schenck 2000). MRI itself drove the development of superconductive magnets to higher fields and gradient switching rates to the point where peripheral nerve stimulation became a possible limiting factor (Cohen *et al* 1990, Irnich and Schmitt 1995, Mansfield and Harvey 1993). More subtle effects such as vertigo and metallic taste became apparent at higher static fields (Cavin *et al* 2006, Glover *et al* 2007). Most of the effects of electric fields that are detectable in humans at low-frequency stem from primary afferent nerve and axon depolarization (Glover *et al* 2007, McRobbie and Foster 1984). In an attempt to understand the causes of such effects, two approaches have been taken. The first is to obtain physiological response data (*in vivo* or *in vitro*) at known delivered currents or magnetic field switching rates (Lovsund *et al* 1980). The latter can then be related to scanner operating parameters. The second approach is to determine the electric field and current density induced in the body using numerical modelling based on a known applied magnetic field and electrical conductivity distribution (Bencsik *et al* 2007, Crozier and Liu 2005, Liu *et al* 2003a, 2003b, Nadeem *et al* 2003, Wang and Eisenberg 1994).

The regulatory bodies have used the physiological data approach to produce directives and guidelines for patients and workers quoting maximum allowed electric fields or current densities, which are dependent on frequency and body location (European Union EMF directive 2004, ICNIRP 1998, IEEE C95.6 2002, WHO 2006). There is currently a lively debate regarding the implications of these regulations on the future of MRI (Gowland 2005, Hill *et al* 2005, Keevil *et al* 2005). To convert the action limits for current density into limits on the magnetic field strength and rate of body movement or the rate of gradient switching does require a number of assumptions to be made and an intensive computational effort. To date the published data from numerical modelling calculations have low spatial resolution. There is therefore a requirement to try and close the gap between realistic situations and their simulation. A number of studies have provided measurements of rates-of-change of magnetic field ($\mathrm{d}B/\mathrm{d}t$) for various movements or tasks around the magnet (Cavin *et al* 2006, Chadwick 2007, Glover *et al* 2007). What is missing is the experimental work which can link the modelling, magnetic fields and induced current density or electric field.

Probes for measuring the electric field in biological systems have been described previously (Tofts and Branston 1991). Electric fields have been measured routinely in phantoms, *in vitro* and *in vivo* for many years over a range of frequencies (Deutsch 1968, Jarzembski *et al* 1970, Kaune and Forsythe 1985, Lang *et al* 1969, McLeod *et al* 1983, Miller 1991, Tay *et al* 1989, Yunokuchi and Cohen 1991). However, there are particular design constraints when using probes to measure the effect of temporally varying magnetic fields. A theoretical approach to understanding these requirements and an experimental justification of the need for the use of a dipole probe arrangement has recently been given by Glover and Bowtell (2007) and is not repeated here.

In this work, true *in vivo* human measurements of induced surface electric fields in the environment of a 3 T scanner are presented for the first time. Two separate dipole probe arrangements were used in the experiments described. The first was suitable for skin surface measurements and contains two orthogonal dipoles. The second, which is based on a single dipole, was used to demonstrate the measurement of electric fields at the tongue

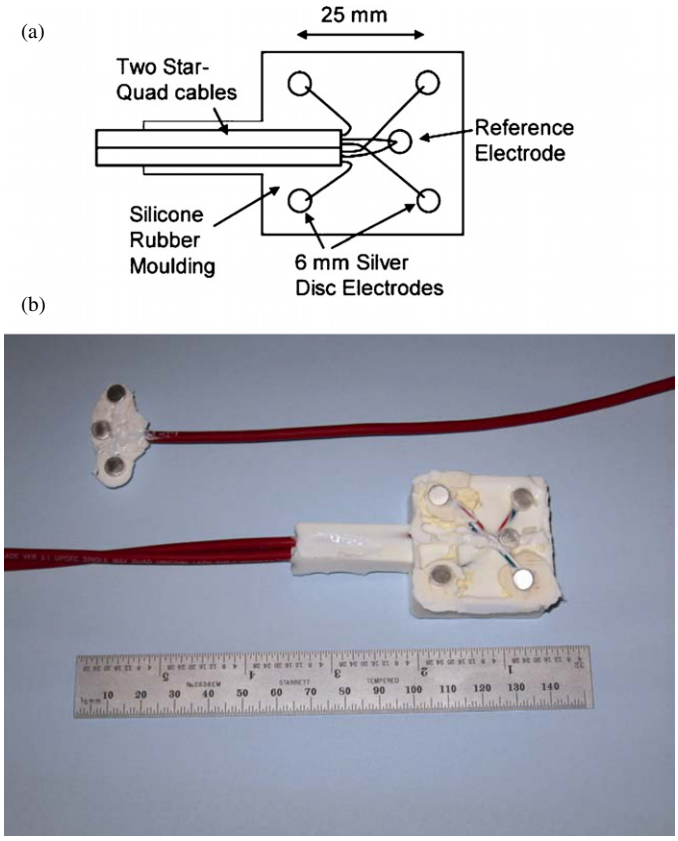

Figure 1. (a) Diagram showing wiring and construction of surface electric field probe moulding. (b) Photograph of the dual-dipole, surface electric field probe and single-dipole, tongue electric field probe.

surface. The concept of a 'geometry factor', which is a constant that relates the rate-of-change of magnetic field to the surface electric field, has also been used to help interpret the measurements.

Methods

Two different electrode configurations were used for the measurements described in this work: a dual-dipole, skin surface arrangement and a smaller, single-dipole surface arrangement applied to the tongue. The primary requirements that must be fulfilled in constructing a dipole probe for the measurement of magnetically induced electric fields are that (i) the electrode separation must be small compared to the length scale over which the current varies and (ii) the leads connecting the electrodes to the cable should run along the straight line between the two electrodes (Glover and Bowtell 2007). Figure 1(a) shows the configuration of the electrodes and the wiring of the cables for the dual-dipole surface probe. Each electrode wire in the diagram is formed by twisting together two (diametrically opposite) cores of the star-quad (Van Damme type 278-801-000) cable. The use of star-quad cable with its low microphonic noise sensitivity was essential for this application. The higher immunity of

this cable to temporally varying magnetic fields compared with conventional twisted pairs means that movement of the cable in the strong magnetic fields of MR scanners does not introduce any unwanted potentials. The electrodes used for measurements on both the skin surface and tongue were silver discs of 6 mm diameter and 0.5 mm thickness (Goodfellow Ltd, Cambridge, UK). The electrodes were embedded in a 12 mm thick, moulded silicone rubber pad. In constructing the probes, the electrodes were first soldered to the cable and then fixed in place by using a 1.6 mm thick PTFE mask with 6.25 mm holes drilled in it at the appropriate locations. Sticky tape on the reverse side of the PTFE sheet temporarily held the discs in place. The PTFE sheet and electrode assembly were then clamped to both a backing sheet and a nylon mould of the desired shape. Mould release agent was used around the edges of the mould and non-corrosive (to metals) silicone rubber (ACC Silicones Ltd, Bridgewater, UK) was injected into the mould in four layers. Each layer was allowed fully to cure before the addition of the next. Note that the photograph of the prototype surface electrode in figure 1(b) shows minor defects in the moulding process which did not affect its performance. After a number of attempts at 'chloriding' the silver electrodes (Geddes *et al* 1969), it was decided that the chloriding process degraded the stability of the contacts with no apparent benefit in low-frequency performance. The electrodes were therefore left as plain silver. The electrode assemblies were calibrated by placing them in a long square-section trough of saline whilst a known 100 Hz alternating electric field was generated by connecting a signal generator across two copper end plates.

The dB/dt probe comprised three coils arranged orthogonally to each other and wound on a small nylon former. Each coil was made up of three turns of 0.8 mm diameter wire wound on a 6 mm diameter former. Star-quad cable was also used for connecting each coil to the amplifier. In order to calibrate these coils, they were placed inside a small solenoidal coil which was driven with an alternating current at 100 Hz and the values of induced EMF were then compared to measurements of RMS magnetic field obtained using a Hall probe flux meter (GM04 Hirst Magnetic Instruments, Falmouth UK).

The electric and magnetic field sensors were interfaced to a BrainVision recorder EEG amplifier and acquisition system (BrainAmp MR plus model, Brain Products, Munich, Germany) which has a sampling rate of 5 kHz. A bandwidth of 1 kHz was selected for the switched gradient measurements, while the frequency range for the low-frequency measurements was 0.1–250 Hz. The amplifier system was optically-isolated and non-magnetic. The EEG amplifier has 32 separate channel amplifiers. A pair of these channels was used in differential mode for each dipole and dB/dt sensor. The BrainAmp designated 'reference' and 'ground' lines were connected together and then to the reference electrode on the dipole sensor via the screen wire of the star-quad cable. Each magnetic field sensor was also referenced to 'ground' via a 10 kΩ resistor.

The measurements were separated into two distinct groups involving (i) low-frequency natural movements and (ii) exposure to switched magnetic fields due to scanner gradient pulses. For the work reported here, a single male subject was used for all measurements (47 year old, 85 kg weight, 183 cm height) in order to maintain consistency of subject geometry. Ethical approval for this study was obtained from Nottingham University Medical School Ethics Committee.

Natural movements

For the first set of measurements, the electric field sensor was fixed to the subject's upper abdomen approximately 10 cm below the sternum. The skin was lightly abraded and cleaned with an acetone–alcohol preparation pad in order to make a good contact with the dermis

layers. Ten20^{TM} conductive EEG paste (D.O. Weaver & Co., Aurora, CO) was applied to each electrode to ensure a stable contact. This paste was sufficiently solid to remain in position and maintain a good mechanical contact between skin and electrode. The electrode pad was secured to the skin using Transpore^{TM} (3M Health Care Ltd, Loughborough, UK) tape and was ready to use in a few minutes. With the sensor attached to the abdomen, a series of three natural movements were performed at the end of the bore of a Philips 3T Achieva scanner which uses a short, actively-shielded magnet (Philips Medical Systems, Eindhoven, Netherlands). The subject was asked to (i) walk forward across the magnet bore and back again without turning; (ii) stand facing the bore on the axis of the magnet and then to rotate plus and minus 90° about the head-foot axis; and (iii) stand, bend and lean into the magnet bore. A further measurement was made with the subject lying on the patient bed whilst it travelled into the scanner during a standard scanner protocol for positioning the subject. In separate measurements, the sensor pad was attached to the forehead of the subject and rotational head movements were performed. Only one measurement was made with this arrangement as the less compressible surface of the forehead made reliable connection difficult. In further measurements, the small single dipole probe (25 mm electrode separation) was placed on the surface of the subject's tongue with the dipole direction being left-to-right. A series of nodding and head-shaking rotations (i.e. rotation of the head about the left–right or head–foot axes) were then carried out with the subject's head positioned at the end of the magnet bore.

Gradient switching

For the alternating magnetic field measurements, the scanner generated a train of echo planar imaging (EPI) sequences having a repeat period of approximately 1 s. A 10 ms gradient pulse with a controlled amplitude and ramp time was added to the start of each EPI sequence. The gradient amplitude of this pulse was initially set to 30 mT m^{-1} with a ramp rise-time of 3 ms which gave a rate-of-rise of gradient of 10 T m^{-1} s^{-1}. The gradient pulse was played out on all three gradient channels X, Y and Z in separate measurements for each of three subject positions. The scanner designates the gradient directions as right–left, anterior–posterior and foot–head respectively for a subject lying supine on the scanner bed. Two sets of measurements were made with the subject lying in the scanner bore with his head at iso-centre. For these measurements, the Philips head Transmit-Receive birdcage coil was used so as to minimize the RF levels in the vicinity of the electrodes (although the EEG system is regularly used within the RF coil safely). The electrode sensor was fixed to either the abdomen, as before, or to the upper chest approximately 10 cm above the sternum. For the two sets of measurements made with the subject in the scanner bore, the sensor was sited approximately either 50 cm or 30 cm from the centre of the gradient coils. In a third set of measurements, the subject stood at the end of the magnet facing into the bore and positioned off-axis in the left–right direction by a distance approximately equal to the bore radius. This brought the abdomen where the sensor was positioned, as close as possible to the gradient coils' windings, with the aim of generating the largest induced electric fields that a subject standing at the end of a scanner could possibly experience. For these measurements, the scanner's rate-of-rise of gradient was increased to 40 T m^{-1} s^{-1} in order to allow reliable measurement of the lower levels of induced electric field. In all of the experiments, the dB/dt sensor was attached to the body of the subject as close as practically possible to the electric field sensor. The 'vertical' axis coil was orientated such that its sensitive axis was parallel to the subject's vertical (foot–head) axis. It was not possible to define fully the orientation of the other coils and these are referred to as the 'transverse' coils.

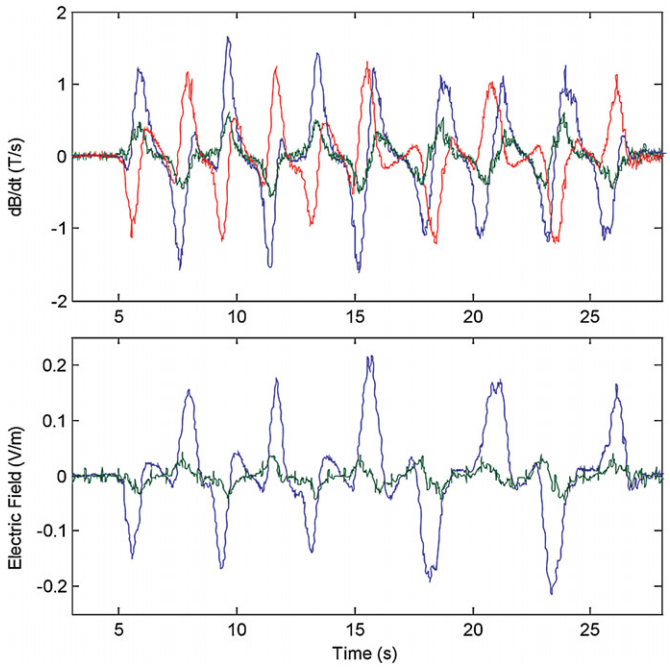

Figure 2. Rate of change of magnetic field (upper) and measured surface electric field (lower) graphs for rotation of the body about the head-foot (vertical) axis at the bore entrance of 3 T magnet. The movement comprised a rotation of 90° clockwise followed by rotation 90° anti-clockwise, repeated three times. The sequence was then repeated, but using 180° rotations. The whole sequence lasted for 30 s. In the upper graph, the red and blue traces show transverse dB/dt components and green shows the vertical component referenced to the body. In the lower graph, the blue trace shows the vertical electric field component and the green trace shows the azimuthal component (around the chest).

Results

In calibrating the electric field sensors the measured potential differences were within 5% of the expected values calculated from the geometry of the electrode arrangement. Hence only small correction factors were required. Although it would be highly desirable to check the sensitivity and frequency response *in vivo*, it was deemed not particularly useful (or safe) to apply very low-frequency currents directly to the subject. The voltages measured using the dipole probes were found to be proportional to dB/dt over frequencies ranging from less than 1 Hz to above 800 Hz, indicating that the sensor operated correctly within this frequency range. The lower limit to the frequency band appeared to be entirely due to the high-pass 0.1 Hz cut-off frequency of the EEG amplifier. The calibration of the dB/dt sensor implied that the effective diameter of each coil winding was approximately 7 mm. The error associated with both electric and magnetic field sensor measurements was estimated to be less than $\pm 5\%$. Although not particularly relevant to this study, it was very useful to be able to observe the electric fields generated by the heart when the sensor was placed on the chest or abdomen (figures 2–4). The presence of the cardiac signal confirmed the correct operation of the sensor and amplifier before commencing subject movements or other measurements. The peak electric field generated by the heart on the surface of the lower abdomen was measured as about 10 mV m^{-1}. The cardiac signal was not seen when the sensor was located on the tongue (figure 5) or head.

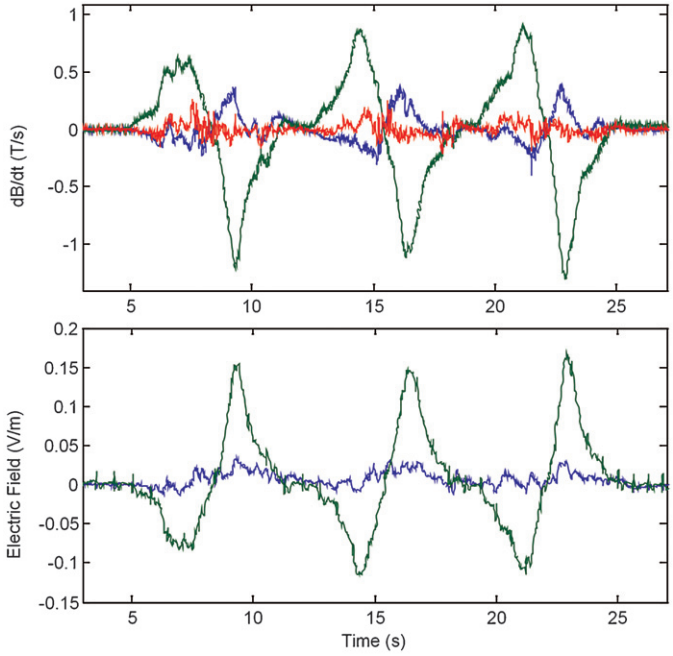

Figure 3. Induced electric field for subject leaning into 3 T magnet. The subject repeated the in-out movement three times over a period of 20 s. The surface probe is attached to the upper abdomen. Trace descriptions as for figure 2.

Figure 2 shows the electric fields induced on the upper abdomen by rotational motion around the subject's vertical axis. The $\mathrm{d}B/\mathrm{d}t$ sensor readings indicated that the transverse components of the changing magnetic field were much larger than the vertical component, as would be expected. The measurement of the electric field shows that the current flow for this type of motion was predominantly in the vertical direction on the surface of the abdomen. The resultant electric field vector components in the vertical and azimuthal (around the abdomen) directions are displayed in figure 2 although the sensor dipoles were actually arranged diagonally on the abdomen. Table 1 summarizes all of the measurements made during natural movement by listing typical peak values of both the electric field and rate-of-change of magnetic field. Both positive and negative peaks were used to derive the values so as to eliminate the slight effects of any dc offsets. The uncertainty given for peak measurements is that derived from the calibration of the probes rather than that caused by the spread of values due to natural variation in the exact body movements that were executed. The column labelled 'Geometric multiplier' shows the mean value $\pm$ the standard error of the constant of proportionality relating the strength of the dominant electric field component to the value of the dominant component of $\mathrm{d}B/\mathrm{d}t$ taken from measurements of a number of instantaneous values of both throughout the recording. The final column of the table indicates the dominant components of the fields which are linked by the geometric multiplier. These components have been identified by visual inspection of the temporal variation of the data.

Figure 3 shows the electric field induced when the subject leant into the magnet three times over a period of 20 s. In this case, the largest component of $\mathrm{d}B/\mathrm{d}t$ is in the vertical axis and the electric field is predominantly directed azimuthally around the body. Figure 4 shows the electric field induced when the subject walked forward and back across the bore of the

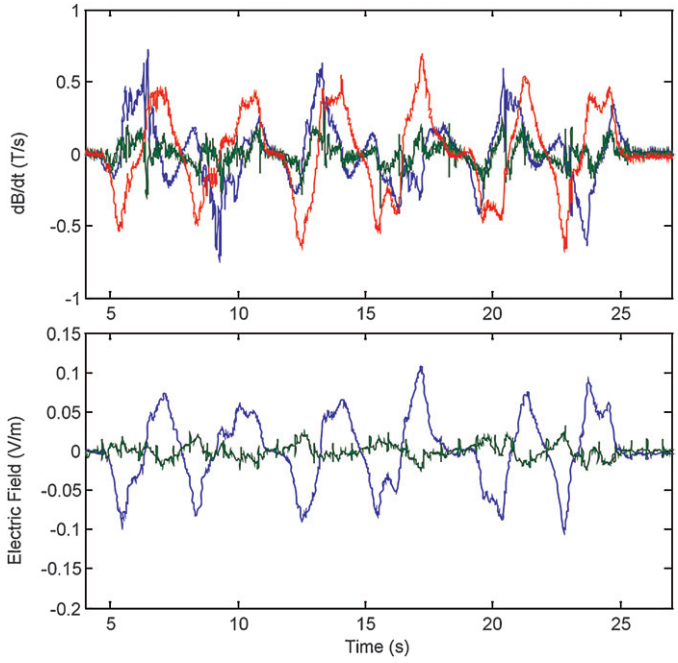

Figure 4. Induced electric field for subject walking forward and back (without turning) six times in front of the magnet bore. The surface probe is attached to the upper abdomen. Trace descriptions as for figure 2.

Table 1. Summary of movements and measurements in magnet fringe fields.

Body region	Sensor location	Action/ movement	Typical Peak dB/dt (T s^{-1})	Typical peak electric field (V m^{-1})	Mean geometric multiplier (m)	Dominant linked field components (dB/dt to E)
Torso	Abdomen	Walking across front of magnet	0.54 ± 0.03	0.085 ± 0.004	0.16 ± 0.01	Transverse to vertical
	Abdomen	Rotating body 90° at bore end	1.08 ± 0.05	0.17 ± 0.01	0.15 ± 0.02	Transverse to vertical
	Abdomen	Standing and bending into magnet bore	1.06 ± 0.05	0.13 ± 0.01	0.13 ± 0.01	Vertical to azimuthal
	Abdomen	On patient bed travelling into magnet	0.82 ± 0.04	0.082 ± 0.04	0.101 ± 0.004	Vertical to azimuthal
Head	Forehead	Rotating head about vertical axis	0.61 ± 0.03	0.046 ± 0.02	0.077 ± 0.003	Transverse to vertical
Mouth	Tongue	Nodding motion of head	2.79 ± 0.3	0.038 ± 0.004	0.015 ± 0.002	Vertical to across tongue

magnet six times. In this case, the vertical component of the electric field and one transverse component of the changing magnetic field were the matching dominant pair. A significant vertical component of dB/dt was also detected, but neither component of the measured electric field showed a strongly matching temporal variation to this component of the rate of change of magnetic field. Figure 5 shows the electric field induced across the tongue by head movements.

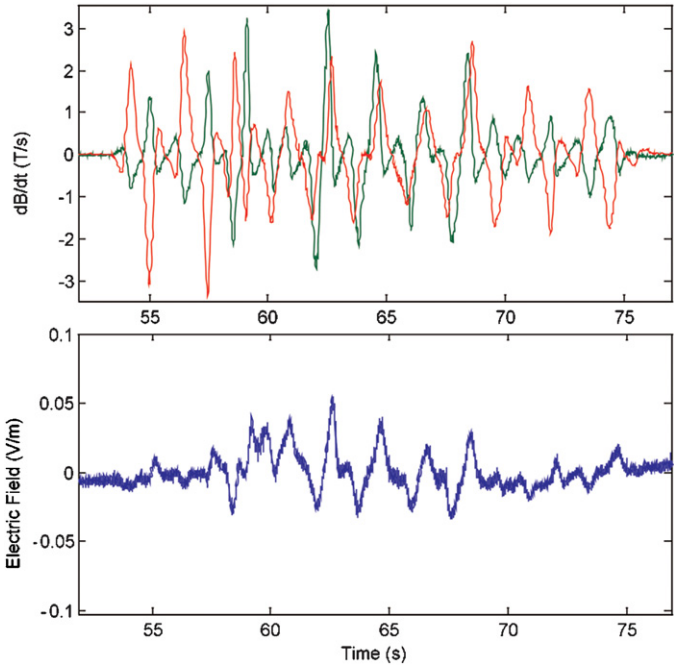

Figure 5. Electric field induced across the surface of the tongue during head movements: (53–57 s)–nodding (57–67 s)–shaking (67–75 s) sequence. The subject knelt in front of the magnet so that his head was level with the axis of the magnet. Trace descriptions as for figure 2, except that the trace from one transverse dB/dt channel has been removed for clarity and only one electric field component was measured.

It can be seen that a significant electric field is only induced across the tongue during the time segment lying between times of 57 and 67 s. This electric field is temporally matched to a changing vertical component of the magnetic field (corresponding to five nodding movements of the head). Head-shaking rotations occurring before the 57 s time point and after the 67 s time point, although producing changes in the transverse components of the magnetic field, did not give rise to a right-to-left electric field on the tongue. This example shows that natural (although vigorous) movement of the head can generate very high peak values of dB/dt.

Figure 6 shows a typical excerpt from the time course of electric and magnetic field variation measured during the execution of an EPI sequence. The largest values of electric field and dB/dt occur during the EPI read-out block during which rates-of-change of gradient around 100 T m^{-1} s^{-1} are applied. Immediately prior to this block the slice selection gradient pulses and (before this) the calibrated 10 ms pulse used for this experiment were played out. Measurements during the EPI read-out block were not used directly in this study for two reasons. First, the scanner scales the gradient levels internally depending on imaging parameters such as field of view and resolution for example. However, the measured dB/dt and electric field values during the EPI read-out block were around ten times higher than the calibrated pulse as expected. Second, slight under-sampling effects can be seen due to the 800 Hz EPI switching and 5000 Hz EEG sampling frequencies. In addition the EPI read-out waveform had frequency components which were higher than the 1000 Hz low-frequency cut-off of the EEG amplifier. A magnified section of the time course showing the time period during which the calibrated pulse is applied is shown on the right of figure 6. Table 2 details values of electric field and dB/dt produced by this pulse. The cardiac potentials were seen on

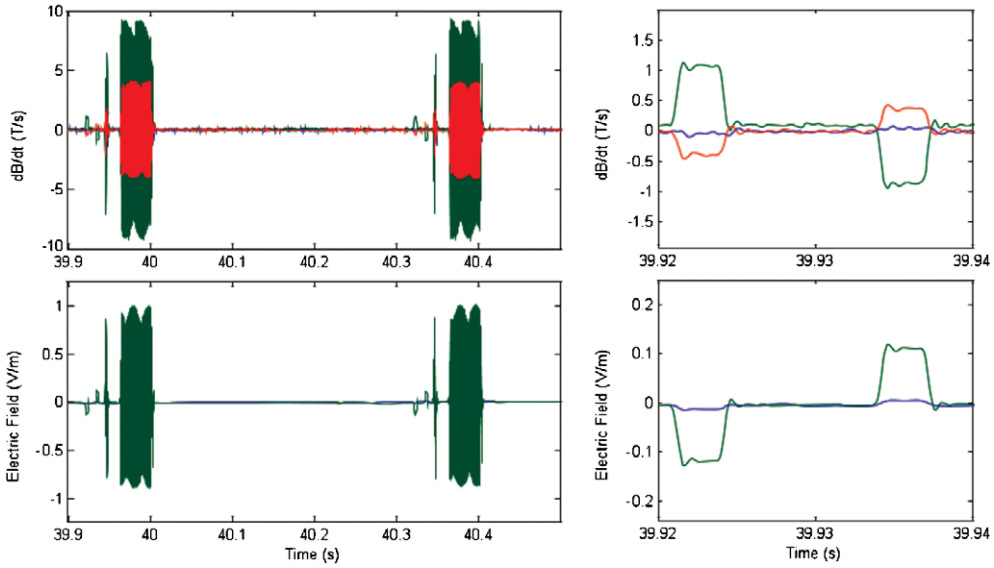

Figure 6. Electric field induced and dB/dt measured with the sensor on the abdomen during echo planar imaging. The data shown here correspond to the Y orientation of the measurement gradient pulse. The calibrated gradient pulse with a 10 T m s^{-1} rise-time can be seen to occur just prior to the slice select and EPI read-out blocks which generate much larger measured fields. Values measured during the application of the calibrated gradient pre-pulse are shown in detail on the right.

Table 2. Summary of induced electric fields in the body due to switched magnetic field gradients. The rise-time of the gradient pulse was set to 10 T m^{-1} s^{-1} except for outside magnet where 40 T m^{-1} s^{-1} was used. In the latter case, the figures in the table have been divided by 4 to allow direct comparison.

Body region and location	Sensor location	Gradient orientation	Peak dB/dt (T s^{-1})	Peak electric field (V m^{-1})	Geometric multiplier (m)	Dominant linked field components (dB/dt to E)
Torso in magnet	Abdomen	Z (foot–head)	1.35 ± 0.07	0.19 ± 0.01	0.14 ± 0.02	Vertical to azimuthal
	Abdomen	X (right–left)	0.505 ± 0.03	0.090 ± 0.005	0.18 ± 0.02	Transverse to vertical
(sensor 50 cm from iso-centre)	Abdomen	Y (anterior–posterior)	0.96 ± 0.05	0.11 ± 0.01	0.12 ± 0.01	Vertical to azimuthal
Torso in magnet	Chest	Z (foot–head)	2.2 ± 0.1	0.30 ± 0.03	0.14 ± 0.02	Vertical to azimuthal
	Chest	X (right–left)	1.44 ± 0.07	0.22 ± 0.01	0.15 ± 0.02	Transverse to vertical
(sensor 30 cm from iso-centre)	Chest	Y (anterior–posterior)	1.64 ± 0.08	0.058 ± 0.003	0.035 ± 0.004	Transverse to azimuthal
Torso outside magnet	Abdomen	Z (foot–head)	0.025 ± 0.002	0.0038 ± 0.0002	0.15 ± 0.04	Vertical to azimuthal
				0.0025 ± 0.0002	0.10 ± 0.02	Vertical to vertical
	Abdomen	X (right–left)	0.055 ± 0.003	0.0033 ± 0.0002	0.06 ± 0.03	Transverse to azimuthal
(Standing at bore edge facing magnet)	Abdomen	Y (anterior–posterior)	0.059 ± 0.03	0.0024 ± 0.0002	0.04 ± 0.02	Vertical to vertical

the electric field traces, but quantitative measurements were taken where these do not interfere. The peak values of the dB/dt and electric field shown in the table for the case where the subject was outside magnet (where a four times larger gradient was used) have been scaled down by a factor of 4 to allow direct comparison with the other measurements. Both electric field component values measured on the abdomen during z-gradient switching (subject outside the magnet) are tabulated in table 2 as these were of similar magnitude.

Discussion

The electrode contact frequency roll-off is certainly well below 1 Hz making the probes used here suitable for natural movement detection. Perhaps one of the main contributions to our success in measuring electric fields induced by movement in static magnetic fields has been the use of high-quality star-quad cable. The high immunity of this cable to voltages resulting from cable movement in magnetic fields leads to a high confidence in the quality of the measurement of the surface currents. This property was also demonstrated by rapidly moving the cable through the magnetic field whilst the sensor was connected to the subject. No induced potentials due to cable movement which were above the physiological and baseline noise of the measurements were observed. The values of peak dB/dt measured in the experiments in which time-varying gradients were applied are consistent with the spatial variation of the magnetic fields due to the gradient coils which were determined from data supplied by the scanner manufacturer. In these experiments, the sensors were positioned outside the region of gradient homogeneity so the absolute field cannot be obtained by simple calculation based on a linear variation of field with position.

One of the most interesting (and surprising) observations is the consistency in the magnitude of the geometric multiplier which was calculated over a range of frequencies and field/subject geometries. Although clearly smaller for the mouth and head, the values for the multiplier relating dB/dt to the electric field in measurements on the chest and abdomen lie mostly in the range of 0.1–0.18 m. The only exception is the chest measurement for *Y*-gradient switching where the coupling is from transverse to azimuthal and the geometry factor takes a much lower value. For a disc of uniform conductivity exposed to a spatially-invariant, orthogonal magnetic field changing in time, the geometry factor is equal to half the disc radius. Hence the geometry factors determined in this work are of similar magnitude to the values expected from torso and head dimensions. If anything, the values are slightly higher than expected, but this could be due to the single point nature of the measurement, the highly non-uniform magnetic fields and the spatial variation of electrical conductivity within the subject's body. In previous work, Irnich and Schmitt (1995) assumed a value of the geometry factor equivalent to 0.16 m to estimate the peak electric fields induced in a body due to MR scanner switched magnetic gradient fields. Their assumption is within the range of values we report here. Comparison with numerical modelling of the electric fields induced in the human body is difficult because of the way the data have been presented in previous publications (Bencsik *et al* 2007, Chadwick 2007, Crozier and Liu 2005). However, peak values for electric field and assumed currents are not dissimilar in overall magnitude to those measured here.

The dermal current can be calculated by assuming a conductivity of 0.4 S m^{-1} (Cheng *et al* 1996). Taking this value would indicate that natural movements around the scanner produce peak values of current density of the order 100 mA m^{-2}. It is worth noting that the subject did not report any perception of vertigo or metallic taste, or experience peripheral nerve stimulation (PNS) during the tests. For the latter to happen the gradients would have to be set to give a rate of rise of field in the region of 200 T m^{-1} s^{-1} within the subject's torso and therefore produce an electric field of order 6 V m^{-1} (Budinger *et al* 1991, Irnich and Schmitt 1995). It was not the intention of this experiment to determine the threshold of physiological effects in this study. However the measured average geometry factor for the torso during body rotation indicates that a rate-of-change of magnetic field exceeding 40 T s^{-1} is required for generation of PNS. A value of this magnitude for dB/dt would be very difficult to achieve in the environment of a clinical MR scanner with natural movements.

Conclusions

This work has shown for the first time that the induced surface electric field vector can be reliably measured *in vivo* within the environment of an MR scanner. The electric field generated on the surface is related to the strength and direction of the rate of change magnetic field by a factor that depends on the geometry of the subject. Values of the geometry factor were found to vary between 0.1 and 0.18 m for measurements on the torso, and are similar in magnitude over a range of frequencies from 0.1 to 800 Hz. The geometry factors for surface electric fields measured on the head and across the tongue are smaller than for the torso, taking values of 0.08 m and 0.015 m respectively. Although proper comparison of our experimental measurements with the predictions of electromagnetic modelling would require the latter to be applied to a precise model of the magnetic field distribution and body geometry that obtained during the experiments, comparison with previously published numerical data corresponding to similar situations indicates that the measured and simulated electric fields are similar in magnitude (Bencsik *et al* 2007, Chadwick 2007, Crozier and Liu 2005).

Using known values of tissue conductivity, the current density under the sensor can be calculated and the measurements reported here show that current densities in excess of regulatory limits may be generated even for moderate natural movements near to a clinical 3 T scanner although the subject did not report any perception of physiological effects. The electric fields induced due to natural movements near to the scanner are much higher than those induced by time-varying fringe fields from the gradient coils in a subject standing still next to the scanner whilst the scanner is operating. Because of the consistent values of geometry multiplier, there is a possibility that a single average value could be used in conjunction with the more easily measured $\mathrm{d}B/\mathrm{d}t$ value to predict maximum electric field and current density within the body.

Acknowledgments

We thank the UK Medical Research and Engineering and Physical Sciences Research Councils for their support of this project (Grant numbers GR/T22445 and G9900259). We thank Ian Thexton and Jeffrey Smith for technical support.

References

Bencsik M, Bowtell R and Bowley R 2007 Electric fields induced in the human body by time-varying magnetic field gradients in MRI: numerical calculations and correlation analysis *Phys. Med. Biol.* **52** 2337–53

Budinger T F, Fischer H, Hentschel D, Reinfelder H E and Schmitt F 1991 Physiological-effects of fast oscillating magnetic-field gradients *J. Comput. Assist. Tomogr.* **15** 909–14

Cavin I D, Glover P M, Bowtell R W and Gowland P A 2006 Thresholds for perceiving a metallic taste at large magnetic field *14th Annual Meeting of the International Society for Magnetic Resonance in Medicine (Seattle, WA)*

Chadwick P 2007 Assessment of electromagnetic fields around magnetic resonance imaging (MRI) equipment UK Health and Safety Executive RR570. http://www.hse.gov.uk/research/rrpdf/rr570.pdf

Chakeres D W and de Vocht F 2005 Static magnetic field effects on human subjects related to magnetic resonance imaging systems *Progr. Biophys. Mol. Biol.* **87** 255–65

Cheng K, Tarjan P P and Mertz P M 1996 Conductivities of pig dermis and subcutaneous fat measured with rectangular pulse electrical current *Bioelectromagnetics* **17** 458–66

Cohen M S, Weisskoff R M, Rzedzian R R and Kantor H L 1990 Sensory stimulation by time-varying magnetic-fields *Magn. Reson. Med.* **14** 409–14

Crozier S and Liu F 2005 Numerical evaluation of the fields induced by body motion in or near high-field MRI scanners *Progr. Biophys. Mol. Biol.* **87** 267–78

Deutsch S 1968 A probe to monitor electroanesthesia current density *IEEE Trans. Biomed. Eng.* **15** 130–1

European Union EMF Directive 2004 /40/EC Minimum health and safety requirements regarding the exposure of workers to the risks arising from physical agents (electromagnetic fields)

Geddes L A, Baker L E and Moore A G 1969 Optimum electrolytic chloriding of silver electrodes *Med. Biol. Eng.* **7** 49–56

Glover P M and Bowtell R 2007 Measurement of electric fields due to time-varying magnetic field gradients using dipole probes *Phys. Med. Biol.* **52** 5119–30

Glover P M, Cavin I D, Qian W, Bowtell R and Gowland P 2007 Magnetic field induced vertigo: a theoretical and experimental investigation *Bioelectromagnetics* **28** 349–61

Gowland P A 2005 Present and future magnetic resonance sources of exposure to static fields *Progr. Biophys. Mol. Biol.* **87** 175–83

Hill D L G, McLeish K and Keevil S F 2005 Impact of electromagnetic field exposure limits in Europe: is the future of interventional MRI safe? *Acad. Radiol.* **12** 1135–42

ICNIRP 1998 Guidelines for limiting exposure to time-varying electric, magnetic, and electromagnetic fields (up to 300 GHz) *Health Phys.* **74** 494–522

IEEE 2002 IEEE standard for Safety Levels with Respect to Human Exposure to Electromagnetic Fields, 0–3 kHz, C95.6-2002 (New York: Institute of Electrical and Electronics Engineers)

Irnich W and Schmitt F 1995 Magnetostimulation in MRI *Magn. Reson. Med.* **33** 619–23

Jarzembski W B, Larson S J and Sances A 1970 Evaluation of specific cerebral impedance and cerebral current density *Ann. New York Acad. Sci.* **170** 476–90

Kangarlu A, Burgess R E, Zhu H, Nakayama T, Hamlin R L, Abduljalil A M and Robitaille P M L 1999 Cognitive, cardiac, and physiological safety studies in ultra high field magnetic resonance imaging *Magn. Reson. Imaging* **17** 1407–16

Kaune W T and Forsythe W C 1985 Current densities measured in human models exposed to 60-Hz electric-fields *Bioelectromagnetics* **6** 13–32

Keevil S F, Gedroyc W, Gowland P, Hill D L G, Leach M O, Ludman C N, McLeish K, McRobbie D W, Razavi R S and Young I R 2005 Electromagnetic field exposure limitation and the future of MRI *Br. J. Radiol.* **78** 973–5

Lang J, Sances A and Larson S J 1969 Determination of specific cerebral impedance and cerebral current density during application of diffuse electrical currents *Med. Biol. Eng.* **7** 517–25

Liu F, Xia L and Crozier S 2003a Influence of magnetically-induced *E*-fields on cardiac electric activity during MRI: a modeling study *Magn. Reson. Med.* **50** 1180–8

Liu F, Zhao H W and Crozier S 2003b Calculation of electric fields induced by body and head motion in high-field MRI *J. Magn. Reson.* **161** 99–107

Lovsund P, Oberg P A and Nilsson S E G 1980 Magnetophosphenes and electrophosphenes—a comparative-study *Med. Biol. Eng. Comput.* **18** 758–64

Mansfield P and Harvey P R 1993 Limits to neural stimulation in echo-planar imaging *Magn. Reson. Med.* **29** 746–58

Mansfield P and Morris P G 1982 *NMR Imaging in Biomedicine* (New York: Academic)

McLeod B R, Pilla A A and Sampsel M W 1983 Electromagnetic-fields induced by Helmholtz aiding coils inside saline-filled boundaries *Bioelectromagnetics* **4** 357–70

McRobbie D and Foster M A 1984 Thresholds for biological effects of time-varying magnetic-fields *Clin. Phys. Physiol. Meas.* **5** 67–78

Miller D L 1991 Miniature-probe measurements of electric-fields and currents induced by a 60-Hz magnetic-field in rat and human models *Bioelectromagnetics* **12** 157–71

Nadeem M, Thorlin T, Gandhi O P and Persson M 2003 Computation of electric and magnetic stimulation in human head using the 3D impedance method *IEEE Trans. Biomed. Eng.* **50** 900–7

Schenck J F 2000 Safety of strong, static magnetic fields *J. Magn. Reson. Imaging* **12** 2–19

Schenck J F, Edelstein W A, Hart H R, Williams C S, Bean C P, Bottomley P A and Redington R W 1983 Switched gradients and rapidly changing magnetic-field hazards in NMR imaging *Med. Phys.* **10** 133–3

Tay G, Chilbert M, Battocletti J, Sances A, Swiontek T and Kurakami C 1989 Measurement of magnetically induced current-density in saline and *in vivo Images Of The Twenty-First Century, Pts 1–6* pp 1167–8

Tofts P S and Branston N M 1991 The measurement of electric-field, and the influence of surface-charge, in magnetic stimulation *Electroencephalogr. Clin. Neurophysiol.* **81** 238–9

Wang W P and Eisenberg S R 1994 A 3-dimensional finite-element method for computing magnetically induced currents in tissues *IEEE Trans. Magn.* **30** 5015–23

WHO 2006 Environmental Health Criteria 232—Static Fields (Geneva: World Health Organisation)

Yunokuchi K and Cohen D 1991 Developing a more focal magnetic stimulator: 2. Fabricating coils and measuring induced current distributions *J. Clin. Neurophysiol.* **8** 112–20